Study and Simulation of the Radiation background of the ATLAS Experiment at CERN using the Monte Carlo method

Maria Lymperaiou

ECE NTUA

Under the supervision of Professor Evangelos Gazis

March 30, 2018

Overview

Introduction

The Standard Model

The Large Hadron Collider (LHC), as well as the detectors on the LHC ring, have been designed in order to answer essential questions of the Standard Model.

The Standard Model of particle physics (SM) describes all of the known fundamental particles along with their interactions: electromagnetism, the weak interaction and the strong interaction. Gravity is not yet included in the Standard Model as it plays no significant role at the energy scale of particle physics.

There are three kinds of elementary particles: leptons, quarks and the force mediators (gauge bosons).

Leptons and Quarks

Leptons are seperated into: e, μ, τ The quarks carry fractional electric charges, $+2e/3$ or $-e/3$. There are six flavours of quarks:

- Up (u)
- Down (d)
- Charm (c)
- Strange (s)
- Top (t)
- Bottom (b)

Introduction

Gauge bosons

- Electromagnetic force (QED): photon
- Weak interaction (EWT): $W^{\pm}$, Z^{0}
- Strong interaction (QCD): gluons
- Gravity: graviton

The Higgs boson

- The mechanism that describes how the particles gain mass requires the existence of a spin zero boson, the Higgs boson, which has been observed by the ATLAS and CMS experiments.
- The Higgs boson has a mass of $126 GeV/c^2$ and a mean lifetime of 1.6*10E–22 sec

Introduction

Other searches:

Supersymmetry

Every particle has its heavier symmetric pair. The particles differ from their respective supersymmetric ones as to the spin by $1/2$.

CP violation

The Big Bang should have created equal amounts of matter and antimatter in the early universe. Nevetheless, everything in universe is made almost entirely of matter.

Quark - gluon plasma

Shortly after the Big Bang, the universe was filled with a soup of particles, dominated by weakly bounded quarks and gluons, moving nearly the speed of light.

Interactions of particles with matter

- Heavy charged particles (Excitation, Ionization, Cherenkov radiation, Transition radiation)
- Electrons (Inelastic scattering with regional electrons, Bremsstrahlung, Moller and Bhabha scattering)
- Photons (Coherent Scattering - Rayleigh, Incoherent scattering - Photoelectric effect, Compton Scattering, Pair production)
- Neutrons (Scattering, Absorption)
- Electromagnetic and Hadronic showers

The Large Hadron Collider

- Inside a circular underground tunnel
- Perimeter: 26.7 km, depth: 50 - 175 m, diameter 3.8 m

Figure: The LHC tunnel

The Large Hadron Collider

Main goals: acceleration of protons and heavy ions. Beam particles are gradually accelerated to obtain the appropriate final energy.

Proton acceleration

1. Protons 'stripped' from their electrons
2. LINAC2: final energy 50 MeV
3. PSB: accelerated to 1.4 GeV
4. PS: 26 GeV
5. LHC: 7 TeV

Heavy Ion acceleration for short periods

1. LINAC3
2. LEIR

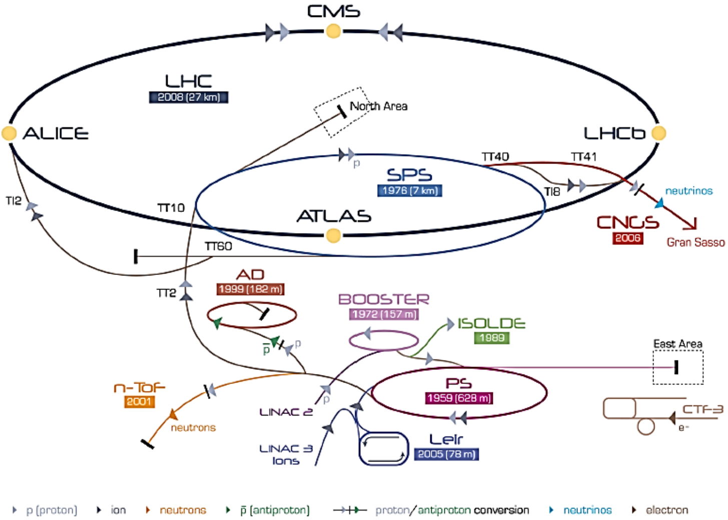

Figure: The LHC complex

The Large Hadron Collider

LHC p-p collisions

Collisions of two proton beams at 4 points

- beams in discrete bunches, interactions in discrete time intervals
- 2808 bunches, $1.15x10^{11}$ protons per bunch
- time between bunch interaction (bunch spacing - BC): 24.95 ns $\approx$ 25 ns
- beam focusing using magnetic lenses of the beam towards the IP
- Inelastic event rate: 600 millions/sec
- 11245 crosses per second $\longrightarrow$ 31.6 millions crosses (average crossing rate)
- 20 inelastic events per crossing, 3550 bunches $\longrightarrow$ 40 million crosses $=$ 40 MHz

The Large Hadron Collider

LHC experiments

- ATLAS (A Toroidal LHC ApparatuS):general purpose
- CMS (Compact Muon Solenoid): general purpose
- ALICE (A Large Ion Collider Experiment): heavy-ion physics and study of quark - gluon plasma
- LHCb: properties of b - quarks and measurements for the CP violation

The Large Hadron Collider

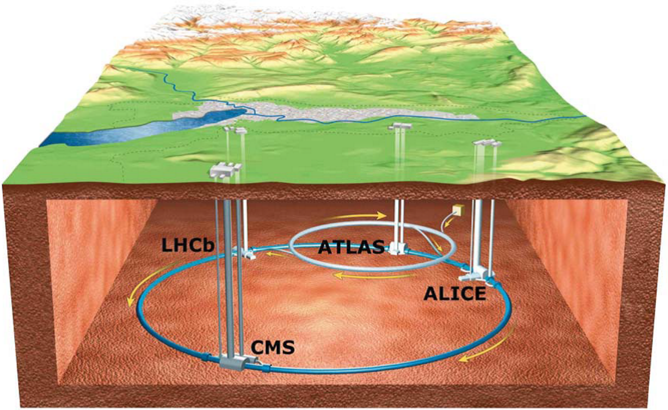

Figure: The four big experiments

The ATLAS experiment

Figure: Aspect of the ATLAS detector

The ATLAS experiment

ATLAS instrumentation

- Inner detector (Pixel Detector, Semiconducting Tracker, Transition Radiation Tracker)
- Calorimeters (Electromagnetic ,Hadronic, Forward)
- Muon Spectrometer (Monitored Drift Tubes, Cathode Strip Chambers, Resistive Plate Chambers, Thin Gap Chambers)
- Forward detectors (LUCID, ALFA, zero degree calorimeter)
- Magnet System (central superconducting solenoid, toroidal air-core)
- Trigger System (Level 1, 2, 3)
- Grid (Tier 0, 1, 2, 3)
- Control System
- Background Monitors

MCNP Simulations

- MCNP (5th edition) was used to simulate the geometry of the ATLAS detector, its materials and the interactions within this detector using a cylindrical source to simulate the proton beam.
- MCNP5 performs the Monte Carlo algorithm to simulate physical interactions and calculate statistically parameters like particle flux on surfaces.
- Time consuming simulations are needed for the accuracy of results.

Source Simulations

- MCNP5 cannot simulate the beam using its actual parameters.
- Thus, we can simulate the conditions within the beampipe, either using a 'point source' on the Interaction Point, or a 'cylindrical source' to represent the proton beam.
- Both cases were tested, and the most accurate was chosen.

Source Simulations

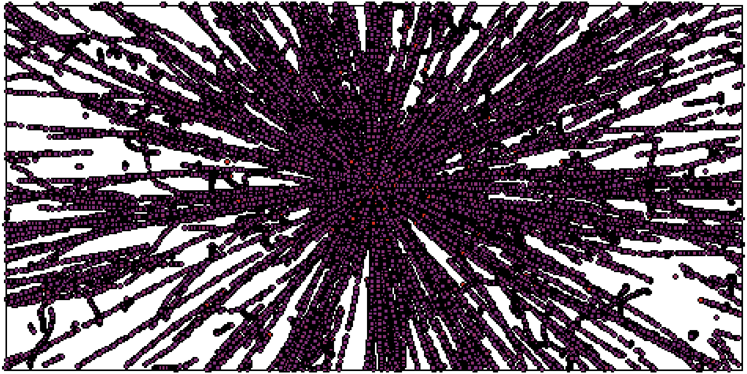

Figure: Particle tracks from a point source placed at (0,0,0) and their tracks after collision.

Source Simulations

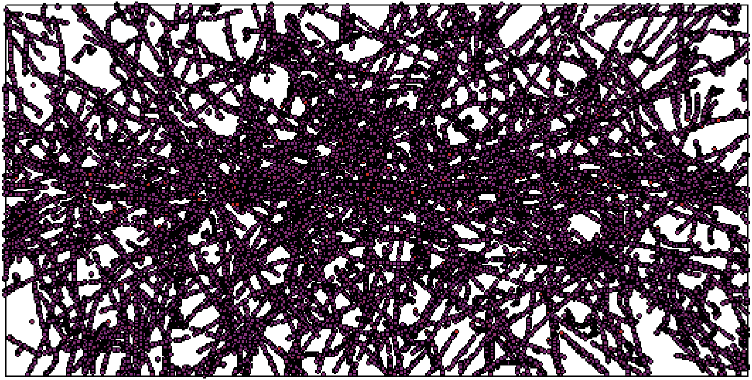

Figure: Source particles and tracks after collisions from particles emmited from a line source. The particles are emmited uniformly.

ATLAS Geometry Simulation

Beampipe

- Region1: z=[-355, 355]cm, r=2.9cm, wall = 2.98 cm (beryllium).
- Region2: z= [-1046.5,-355]cm and z=[355, 1046.5] cm, r=2.9 cm, wall = 2.98 cm (stainless steel).
- Region 3: z= [-1050.7,- 1046.5]cm and z=[1046.5, 1050.7] cm, r = 4cm, wall = 4.1 cm (stainless steel).
- Region 4: z= [-1441.6,- 1050.7]cm and z=[1050.7, 1441.6] cm, r = 6 cm, wall = 6.15 cm (stainless steel).
- Region 5: z= [-1888, -1441.6] cm and z = [1441.6, 1888] cm, r=1.7 cm wall = 3 cm (copper).

ATLAS Geometry Simulation

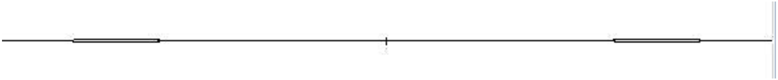

Figure: Design of the ATLAS beampipe

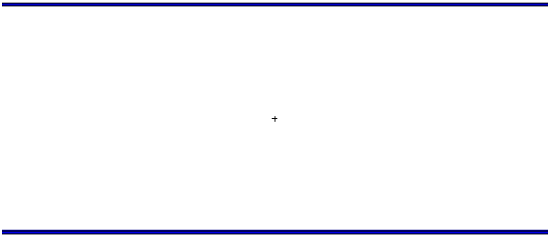

Figure: Zoom towards the IP. The material of the wall (beryllium) is indicated with blue color. Vacuum in the inside is indicated with white.

ATLAS Geometry Simulation

Inner Detector

Subdetector	Z (cm)	R (cm)	Material
Pixel	309.2	4.55-24.2	Silicon
SCT barrel	80.5	25.5-54.9	Silicon
SCT end - caps	81-279.7	25.1-61	Silicon
TRT barrel	78	55.4-108.2	Xenon
TRT end - caps	82.7-274.4	61.7-110.6	Xenon

ATLAS Geometry Simulation

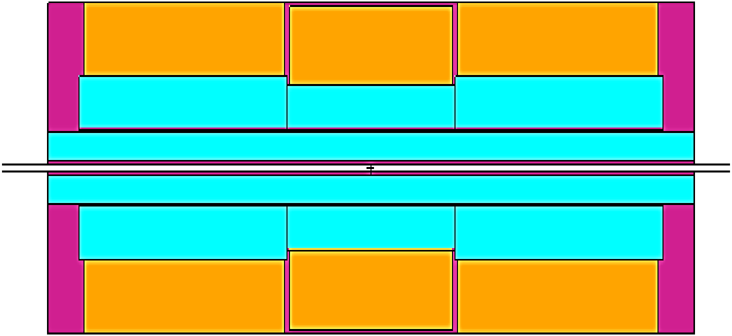

Figure: Design of the Inner detector subsystems.

Calorimeters

Subdetector	Z (cm)	R (cm)	Material
EM Calorimeter (Barrel)	-309.2-309.2	200	Lead
Forward Calorimeter	500-600	25	Lead
EM-Had Calorimeter	350-650	25.1-61	Lead
Hadronic Calorimeter Barrel	-309.2-309.2	400	Stainless Steel
Hadronic Calorimeter End-caps	350-650	400	Stainless Steel

ATLAS Geometry Simulation

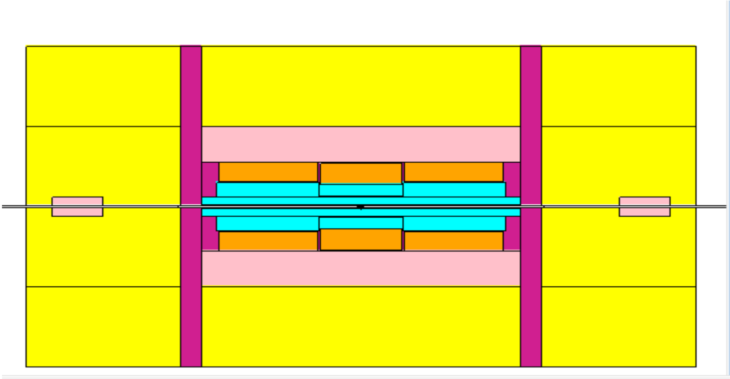

Figure: Design of the Calorimeters. Light pink is used for the lead and yellow for the stainless steel.

Shielding

Subdetector	Z (cm)	R (cm)	Material
JD shielding	800-1300	50	Stainless Steel
JT Cu Shielding	650-800	50	Copper
JF Iron Shielding -1-	1300-1800	100	Iron
TAS collimator	1888-2188	20	Copper
Quadrupole	2200-2400	20	Titanium Alloy (Grade 5)
JF Iron Shielding -2-	1800-2188	200	Iron
JF Iron Shielding -3-	2188-2400	100	Iron
JN Shielding -1-	2188-2300	250	Cast Iron
JN Shielding -2-	2388-2400	300	Cast Iron

- Superconducting Magnet: $z=[800, 1300]$ cm, $r=500$ cm around JT Cu Shielding, material: Titanium Alloy (Grade 5).

ATLAS Geometry Simulation

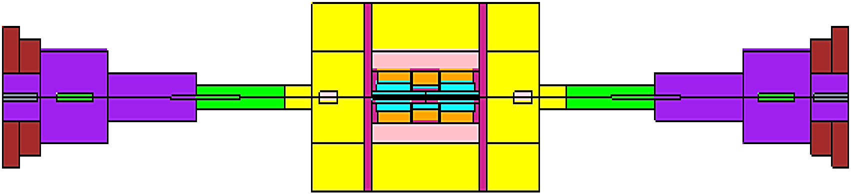

Figure: ATLAS beampipe, ID, Calorimeters and Shielding.

ATLAS Geometry Simulation

Muon Spectrometer

Subdetector	Z (cm)	R (cm)	Material
CSC	650-800	50-200	Argon
Small Wheel	650-800	600	Al, Ar
Muon Inner Barrel	-650-650	500-550	Al, Ar
RPCs	-900-900	770	tetrafluroethane
Muon Medium Barrel	-900-900	700-750	Al, Ar
RPCs	-900-900	990	tetrafluroethane
Muon Outer Barrel 1	-1200-1200	920-990	Al, Ar
RPCs	2188-2300	250	tetrafluroethane
Muon End Cap	100-1075	120-1100	Al, Ar
Muon Medium End Cap	1300-1380	120-1100	IAl, Arron
TGCs (EML) 1	1390-1420	200-1200	Co_2
TGCs (EML) 2	1430-1460	200-1200	Co_2

Figure: MDTs for the BIL.

Figure: Zoomed aspect of the BIL station. The wall of the MDTs made of aluminium is represented by light brown.

ATLAS Geometry Simulation

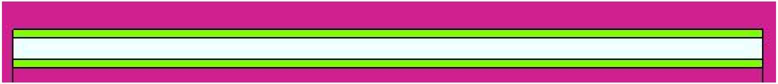

Figure: RPCs and MDTs for the BML.

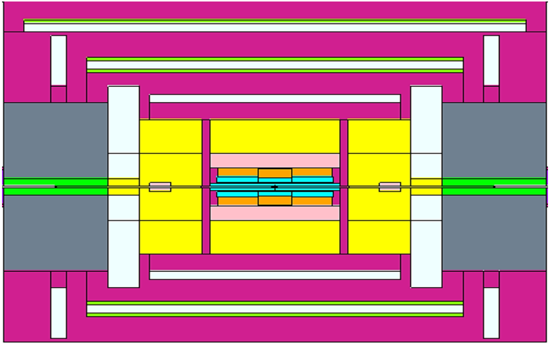

Figure: Muon barrel stations, SW and EEL.

ATLAS Geometry Simulation

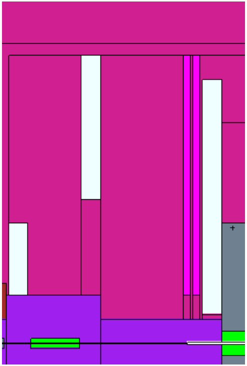

(a) Muon end cap stations

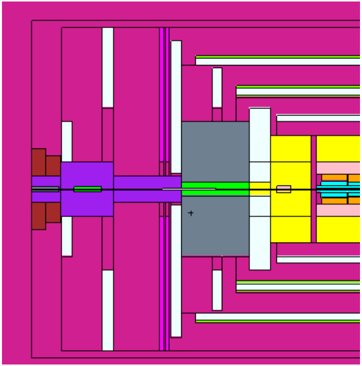

(b) Half of the ATLAS detector, where all the muon stations are shown

ATLAS Geometry Simulation

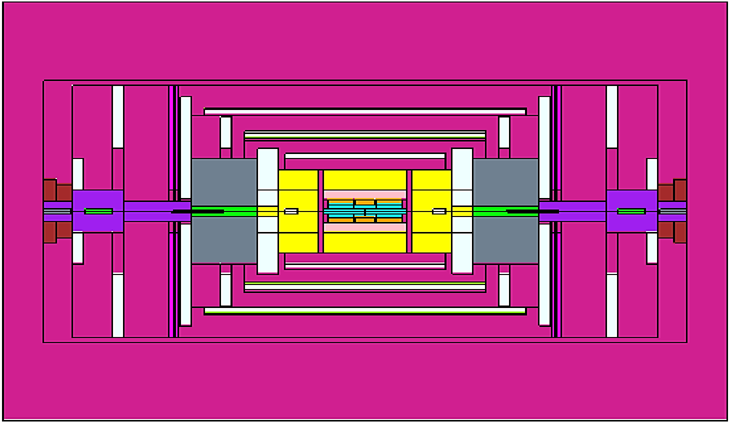

Figure: The ATLAS detector with its cavern.

Source choice

The cylindrical source proved to give more accurate results (comparing to actual measurements on site) comparing to the point source, which was resulting in zero values at the outer regions. So, this source was used for the following measurements.

Photon Measurements in the ATLAS detector

Average surface and cell flux and were measured on every surface of the previous geometry. All the results are expressed as number of particles per cm^2.

Those simulations were executing using 1440 minutes of CPU time.

The measurements below were taken using the MCNP analog simulation.

Photon Measurements in the ATLAS detector

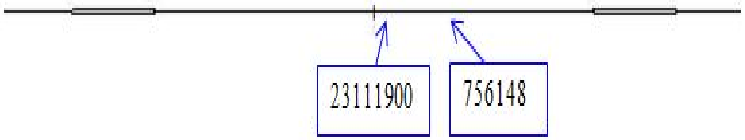

Figure: Photon fluxes in the beampipe

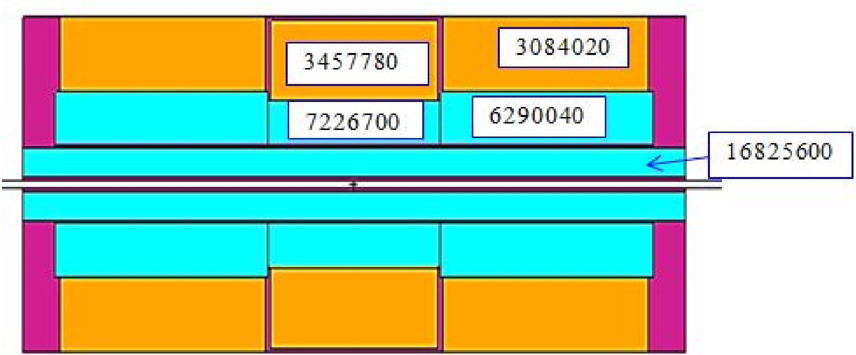

Figure: Photon fluxes in the ID

Photon Measurements in the ATLAS detector

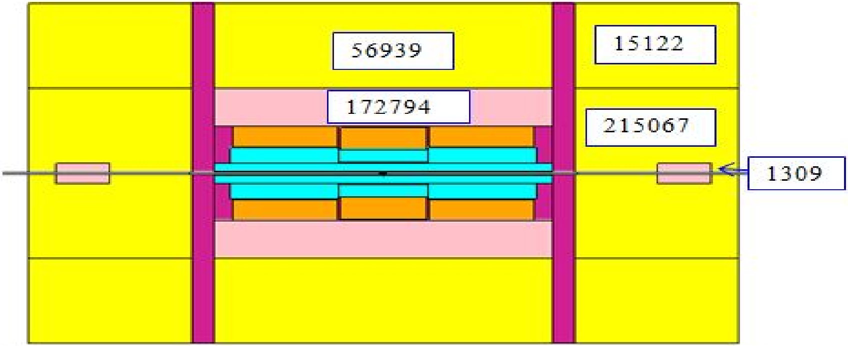

Figure: Photon fluxes in the Calorimeters

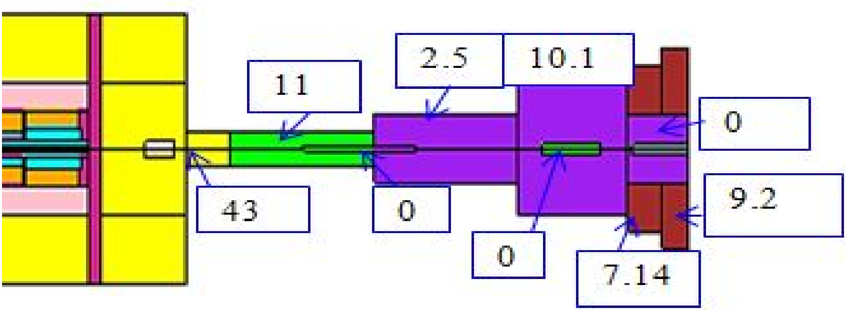

Figure: Photon fluxes in the Shielding regions

Photon Measurements in the ATLAS detector

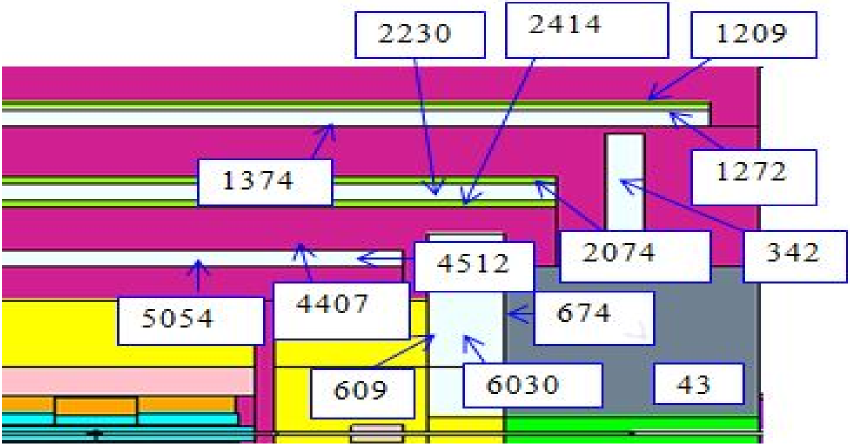

Figure: Photon fluxes in Muon stations

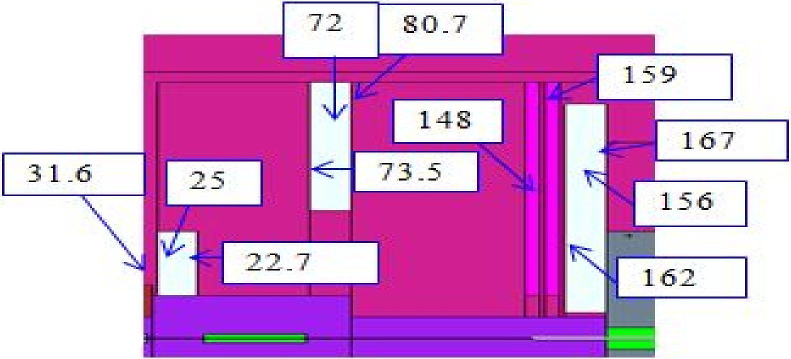

Figure: Photon fluxes in the Muon end - caps

Results

- Comparing to official results obtained through other software packages (mainly FLUKA), the measurements above were accurate enough in most regions.
- Outer regions seem to be less accurate.
- To achieve results even closer to the real ones, even for the 'difficult' outer regions, more advanced computational methods needed to be used.
- MCNP5 non-analog technique was tested.

Non-analog method evaluation

- Make interactions in the outer regions more likely. In the meantime, assign each particle a 'weight', which will be decreased while moving to the outer regions, so that the statistics are not biased.
- First, particle population in each cell needs to be measured, and the ratio of neighbouring cells is better to result in constant population, ie not many particles are lost.
- Then, a new simulation code needs to be built. In this case, outer cells have higher possibility of interaction.
- This method was implemented first in the simplest way. One neighbouring cell was used each time: the chosen neighbour was the outer adjusted cell with which our current one has the maximum overlap.

Non-analog method evaluation

- It was observed that the fluxes when using the non-analog technique are close enough to the analog ones.
- However, the difference between analog and non-analog values is not significant in this case.
- Future improvement: Use a more complex cell population function for the non analog simulation; a most accurate function should take into account more than one neighbouring cells, resulting in a more realistic new cell population.

Background Consequences

- ID: damage to silicon devices, induced ionization
- Calorimeters: signal and safety problems
- Muon stations: reduced lifetime reduced muon track-finding efficiency
- Trigger system: fake triggers, uncorrelated noise hits

The End

Backup slides

1. Heavy charged particles

Excitation

e^- transitions from their initial state to a higher energy state

Ionization

e^- transitions in the continuum. An electron-ion pair is created.

Cherenkov radiation

It is emitted when a charged particle is passing through a dielectric medium at a speed greater than the phase velocity of light in this medium.

Transition radiation

It is emitted when a charged particle penetrates the interface of two media with different electrical properties.

2. Electrons

Inelastic scattering with regional electrons

During the inelastic scattering of e^- excitation and ionization phenomena due to Coulomb field are noted, resulting in energy loss and deviation from their initial trajectory.

Bremsstrahlung

Bremsstrahlung is electromagnetic radiation produced by the deceleration of an e^- when deflected by the atomic nucleus.

Moller and Bhabha scattering

Moller and Bhabha involve interactions between e^- or e^+ with atomic e^-. Moller scattering represents the repulsion of the two e^-. Bhabha scattering represents the attraction between an e^- and a e^+.

3. Photons

Coherent Scattering - Raylight

The incident photon is absorbed and re-emitted immediately without energy loss, only change of direction.

Incoherent scattering - Photoelectric effect

A photo - electron absorbs all the energy of the photon acquiring kinetic energy and an ionized atom is created in the absorber.

Compton Scattering

Describes the inelastic scattering of a γ at an angle θ of an atomic e^-.

Pair production

A γ converts into an e^-–e^+ pair.

4. Neutrons

The possibility of neutron interactions with certain nuclei depends on the type of the material and the neutron energy. They can travel far enough in matter without any interaction.

Neutron Interactions

- Scattering: Elastic, inelastic or non-elastic neutron nucleus scattering
- Absorption: Absorption with γ emission, absorption with charged particle emission, absorption with emission of several neutrons, nuclear fission, hadron jet production

5. Electromagnetic and Hadronic showers

Electromagnetic showers

A γ or e^- of energy higher to a critical energy threshold that enters a material can cause cascade of secondary e^- and γ.

Hadronic showers

A hadronic shower is generated via the strong interaction of a hadron with the nuclei of the atoms of the material.

Basic Simulations

Cylindrical Geometries

- Co-60 source at (0,0,0)
- Length: 50 m on the x-axis, radius 12.5 m, filled with air

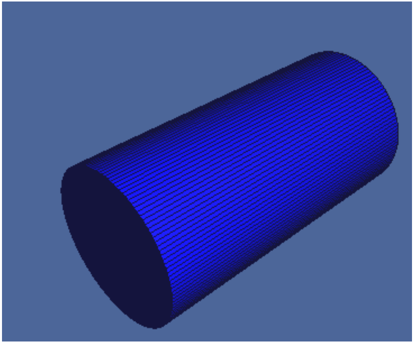

Figure: Simulated cylinder with MCNP (3D plot). [Vised]

Basic Simulations

Surface	**Flux/sp**	**Flux (2 sp)**
Cylinder	2.87071 E-08	5.74142 -08
Right base	1.12482 E-08	2.24964 -08
Left base	1.15430 E-08	2.3086 -08

Table: Photon flux in a cylinder simulated by MCNP

Simulations

Results

- Cylinder filled with air: the flux on each surface depends strongly on the number of emmited source particles and not on the energy
- The energy of these particles relocates the flux spectrum
- More energetic particles form straighter tracks and they can travel further.
- The number of the existing sources can be a very influencing factor, when the relocation of the source can influence slightly only the fluxes on the the approaching surfaces.
- In different materials the energy of the source influences the induced flux on surfaces.

Source Simulations

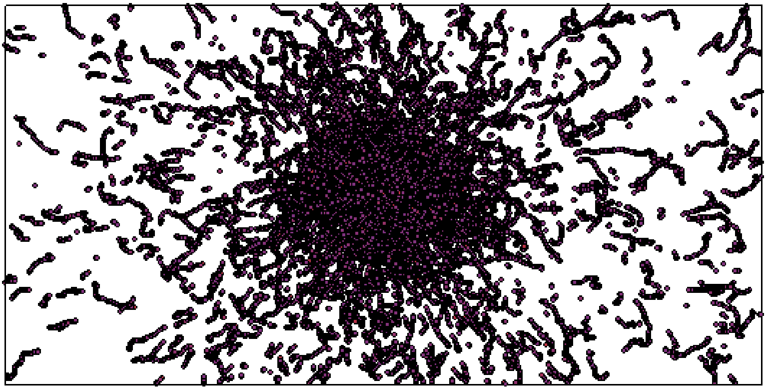

Figure: Particle tracks from three Co-60 sources placed at (-20,0,0), (0,0,0),(20,0,0) respectively and their tracks after collision.

Source Simulations

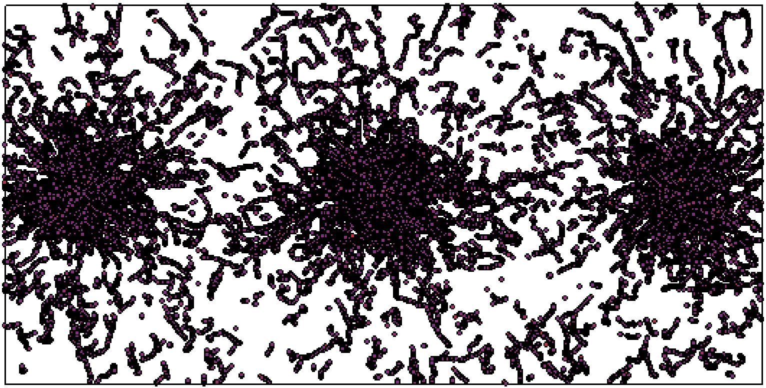

Figure: Particle tracks from three Co-60 sources placed at (-2000,0,0), (0,0,0),(2000,0,0) respectively and their tracks after collision.

Simulations

Figure: Particle tracks from a 10 MeV source placed at (2000,0,0) and their tracks after collision

Simulations

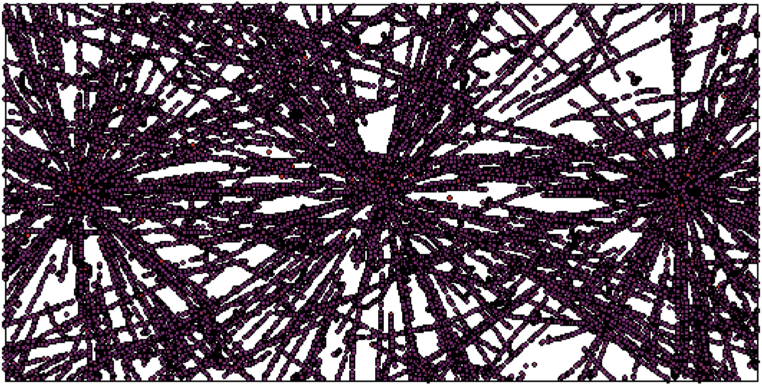

Figure: Particle tracks from three 30 MeV sources placed at (-2000,0,0), (0,0,0), (2000,0,0) respectively and their tracks after collisions

Material Simulations

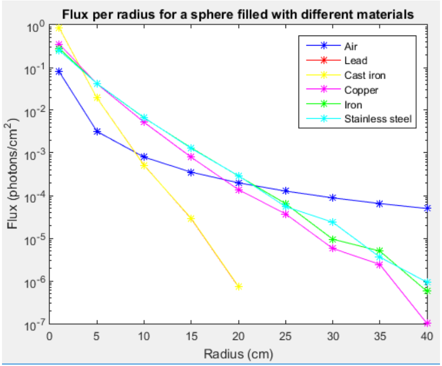

(a) Attenuation of photon fluxes depending on the distance from the source.

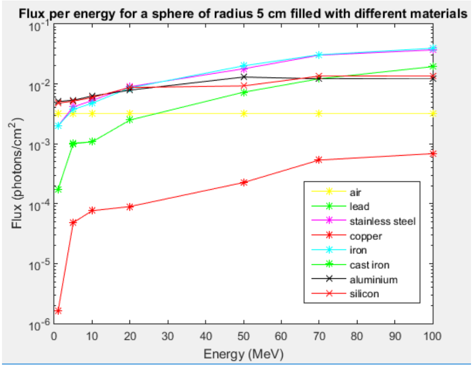

(b) Photon flux for sources of increasing energy.

Figure: Photon fluxes in different materials used in ATLAS shielding regions.

Source Simulations

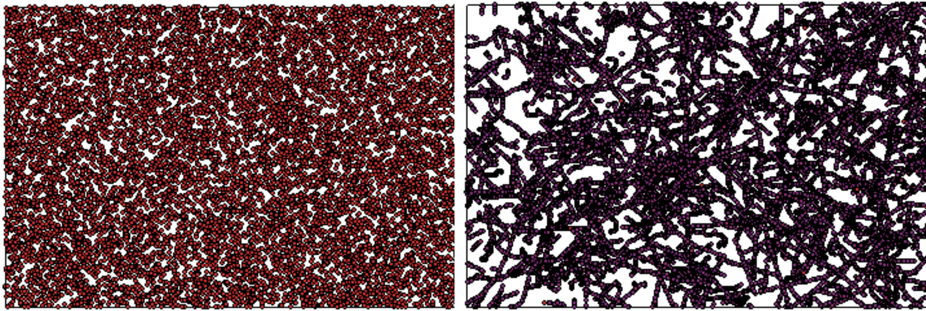

(a) Distribution of source particles (b) Particle tracks after collisions

Figure: 5 MeV cylindrical volume source (radius 12.5m , length 50 m)